

30 September 2004

International weekly journal of science

# nature

£10.00

www.nature.com/nature

## Dream beam

The dawn of compact particle accelerators

### Disease control

Europe plays catch-up

### The Earth's hum

Sounds of air and sea

### Protein folding

Escape from the ribosome

### Human ancestry

One from all and all from one

**technology feature** RNA interference



nature

431, 491-612 30 September 2004

www.nature.com/nature

no. 7008

8pg

the plasma is sufficiently short, then one can extract this monoenergetic bunch, before further wave-breaking of plasma oscillations behind the first causes an increased 'dark-current' of lower-energy electrons (marked (3) in Fig. 5). Indeed, in some simulations this 'dark-current' is found to be greatly reduced if the trailing wake is sufficiently perturbed to prevent efficient trapping and acceleration.

In the simulation shown, the end of the plasma (at  $t = 6.6$  ps) is sufficiently close that many of the monoenergetic features remain as they leave the plasma. If the plasma is too long, then the electrons begin to enter a decelerating part of the plasma wave and as a result experience longitudinal energy spread, as can be observed at (4) in Fig. 5. For higher densities, or longer plasmas, this dephasing is complete, and a Maxwellian electron energy spectrum results. Such dephasing has been the case in most previous laser-based acceleration experiments, explaining why such features have not been seen before. However, with the right combination of laser pulse length ( $c\tau \approx \lambda_p$ ), focal spot size, plasma density and interaction length, monoenergetic features such as that in Fig. 3 are the principal characteristic of the spectrum of relativistic electrons in both simulations and experiment. □

Received 26 May; accepted 18 August 2004; doi:10.1038/nature02939.

1. Perry, M. D. & Mourou, G. Terawatt to petawatt subpicosecond lasers. *Science* **264**, 917–924 (1994).
2. Key, M. H. *et al.* Hot electron production and heating by hot electrons in fast ignitor research. *Phys. Plasmas* **5**, 1966–1972 (1998).
3. Tajima, T. & Dawson, J. Laser electron accelerator. *Phys. Rev. Lett.* **43**, 267–270 (1979).
4. Joshi, C. & Katsouleas, T. Plasma accelerators at the energy frontier and on tabletops. *Phys. Today* **56**, 47–53 (2003).
5. Esarey, E., Sprangle, P., Krall, J. & Ting, A. Overview of plasma-based accelerator concepts. *IEEE Trans. Plasma Sci.* **24**, 252–288 (1996).
6. Wagner, R., Chen, S. Y., Maksimchuk, A. & Umstadter, D. Electron acceleration by a laser wakefield in a relativistically self-guided channel. *Phys. Rev. Lett.* **78**, 3125–3128 (1997).
7. Ting, A. *et al.* Plasma wakefield generation and electron acceleration in a self-modulated laser wakefield accelerator experiment. *Phys. Plasmas* **4**, 1889–1899 (1997).
8. Tzeng, K. C. & Mori, W. B. Suppression of electron ponderomotive blowout and relativistic self-focusing by the occurrence of Raman scattering and plasma heating. *Phys. Rev. Lett.* **81**, 104–107 (1998).
9. Modena, A. *et al.* Electron acceleration from the breaking of relativistic plasma waves. *Nature* **377**, 606–608 (1995).
10. Santala, M. I. K. *et al.* Observation of a hot high-current electron beam from a self-modulated laser wakefield accelerator. *Phys. Rev. Lett.* **86**, 1227–1230 (2001).
11. Pukhov, A. & Meyer-ter-Vehn, J. Laser wake field acceleration: the highly non-linear broken-wave regime. *Appl. Phys. B* **74**, 355–361 (2002).
12. Clark, E. L. *et al.* Measurements of energetic proton transport through magnetized plasma from intense laser interactions with solids. *Phys. Rev. Lett.* **84**, 670–673 (2000).
13. Edwards, R. D. *et al.* Characterization of a gamma-ray source based on a laser-plasma accelerator with applications to radiography. *Appl. Phys. Lett.* **80**, 2129–2131 (2002).
14. Malka, V. *et al.* Electron acceleration by a wake field forced by an intense ultrashort laser pulse. *Science* **298**, 1596–1600 (2002).
15. Pukhov, A., Sheng, Z. M. & Meyer-ter-Vehn, J. Particle acceleration in relativistic laser channels. *Phys. Plasmas* **6**, 2847–2854 (1999).
16. Mangles, S. P. D. *et al.* Electron acceleration to 350 MeV due to the direct interaction of an ultra-intense laser pulse with an underdense plasma. *Phys. Rev. Lett.* (submitted).
17. Umstadter, D. Review of physics and applications of relativistic plasmas driven by ultra-intense lasers. *Phys. Plasmas* **8**, 1774–1785 (2001).
18. Umstadter, D., Kim, J. K. & Dodd, E. Laser injection of ultrashort electron pulses into wakefield plasma waves. *Phys. Rev. Lett.* **76**, 2073–2076 (1996).
19. Amiranoff, F. *et al.* Observation of laser wakefield acceleration of electrons. *Phys. Rev. Lett.* **81**, 995–998 (1998).
20. Sprangle, P., Esarey, E. & Ting, A. Nonlinear interaction of intense laser pulses in plasmas. *Phys. Rev. A* **41**, 4463–4467 (1990).
21. Bulanov, S. V., Kirsanov, V. I. & Sakharov, A. S. Excitation of ultrarelativistic plasma waves by pulse of electromagnetic radiation. *JETP Lett.* **50**, 198–201 (1989).
22. Bereziani, V. I. & Murusidze, I. G. Relativistic wake-field generation by an intense laser-pulse in a plasma. *Phys. Lett. A* **148**, 338–340 (1990).
23. Sprangle, P., Esarey, E., Ting, A. & Joyce, G. Laser wakefield acceleration and relativistic optical guiding. *Appl. Phys. Lett.* **53**, 2146–2148 (1988).
24. Akhiezer, A. I. & Polovin, R. V. Theory of wave motion of an electron plasma. *JETP* **3**, 696–705 (1956).
25. Fonseca, R. A. *et al.* *Lecture Notes in Computer Science* Vol. 2329, III-342 (Springer, Heidelberg, 2002).
26. Faure, J. *et al.* Effects of pulse duration on self-focusing of ultra-short lasers in underdense plasmas. *Phys. Plasmas* **9**, 756–759 (2002).

**Acknowledgements** This work was supported by the UK EPSRC and RCUK. We thank the OSIRIS consortium (UCLA/IST Lisboa/USC) for the use of OSIRIS, and S. Karsch for discussions.

**Competing interests statement** The authors declare that they have no competing financial interests.

**Correspondence** and requests for materials should be addressed to S.M. (stuart.mangles@imperial.ac.uk).

## High-quality electron beams from a laser wakefield accelerator using plasma-channel guiding

C. G. R. Geddes<sup>1,2</sup>, Cs. Toth<sup>1</sup>, J. van Tilborg<sup>1,3</sup>, E. Esarey<sup>1</sup>, C. B. Schroeder<sup>1</sup>, D. Bruhwiler<sup>4</sup>, C. Nieter<sup>4</sup>, J. Cary<sup>4,5</sup> & W. P. Leemans<sup>1</sup>

<sup>1</sup>Lawrence Berkeley National Laboratory, 1 Cyclotron Road, Berkeley, California 94720, USA

<sup>2</sup>University of California, Berkeley, California 94720, USA

<sup>3</sup>Technische Universiteit Eindhoven, Postbus 513, 5600 MB Eindhoven, the Netherlands

<sup>4</sup>Tech-X Corporation, 5621 Arapahoe Ave. Suite A, Boulder, Colorado 80303, USA

<sup>5</sup>University of Colorado, Boulder, Colorado 80309, USA

Laser-driven accelerators, in which particles are accelerated by the electric field of a plasma wave (the wakefield) driven by an intense laser, have demonstrated accelerating electric fields of hundreds of  $\text{GV m}^{-1}$  (refs 1–3). These fields are thousands of times greater than those achievable in conventional radio-frequency accelerators, spurring interest in laser accelerators<sup>4,5</sup> as compact next-generation sources of energetic electrons and radiation. To date, however, acceleration distances have been severely limited by the lack of a controllable method for extending the propagation distance of the focused laser pulse. The ensuing short acceleration distance results in low-energy beams with 100 per cent electron energy spread<sup>1–3</sup>, which limits potential applications. Here we demonstrate a laser accelerator that produces electron beams with an energy spread of a few per cent, low emittance and increased energy (more than  $10^9$  electrons above 80 MeV). Our technique involves the use of a preformed plasma density channel to guide a relativistically intense laser, resulting in a longer propagation distance. The results open the way for compact and tunable high-brightness sources of electrons and radiation.

Previous laser driven plasma acceleration experiments have used a single intense ( $10^{18}$ – $10^{19}$   $\text{W cm}^{-2}$ ) laser pulse propagating in the plasma formed when the front edge of the pulse ionized the gas plume emanating from a jet. The laser power was above the critical power for self-focusing and the laser pulse length exceeded the plasma period<sup>6</sup>. In this so-called self-modulated wakefield regime<sup>6</sup>, some self-guiding of the laser pulse occurs owing to relativistic modification of the plasma refractive index, but the laser pulse is highly unstable<sup>7</sup>. Large plasma waves, or wakes, can be driven by the radiation pressure of the intense laser, but the propagation length is limited to little more than the diffraction or Rayleigh length,  $Z_R$  (refs 5, 8). The best results have hence been obtained by increasing the laser spot size to increase  $Z_R$ , requiring ever greater laser power, but this approach has still been limited to distances of a few hundred micrometres (ref. 8). Plasma electrons were trapped and accelerated in the resulting high-amplitude plasma wave, and electron bunches with 100% energy spread and an exponentially small fraction of electrons at high energy were observed. For example, using a 32 TW

laser, bunches with more than  $10^{10}$  electrons were produced but less than 1% were above 60 MeV (ref. 2). The beam divergence was typically greater than 50 mrad full-width at half maximum (FWHM). Whereas these beams are useful for some users<sup>9,10</sup>, many applications, including high-energy physics and radiation sources, require monoenergetic beams (1% energy spread or less) with at least  $10^9$  electrons<sup>11–15</sup>.

In the experiments reported here, a preformed plasma channel, with a radially symmetric density profile that has a minimum on the laser propagation axis, was used to guide the ultra-intense drive laser pulse, circumventing the limits imposed by diffraction<sup>14</sup>. For optimum acceleration, the accelerator length should be matched to the dephasing length, which is the distance it takes the accelerated electrons to outrun the plasma wave and slip into decelerating phase<sup>15</sup>. At high densities, where the laser pulse length is longer than the plasma wavelength, the laser can self-modulate, resulting in large plasma waves that trap particles from the bulk plasma. In a distance of the order of 2 mm, peak energy gain can be of the order of a few hundred MeV (ref. 2). With controlled injection<sup>16,17</sup>, lower densities could be used in the future. The dephasing length and maximum energy increase as density decreases, so that accelerator lengths of several cm and energies up to several GeV per stage are then possible<sup>5</sup>. To reach high intensities with a typical 10 TW peak power laser system operating at 800 nm, the laser pulse must be focused to spot sizes near  $8\ \mu\text{m}$ , giving  $Z_R \approx 200\ \mu\text{m}$  and necessitating guiding over many  $Z_R$  in order to reach the dephasing condition and high energies. A parabolic transverse density profile can be matched to guide a gaussian laser mode without distortion in the low intensity limit, and guiding has been previously demonstrated<sup>18–21</sup> over many  $Z_R$  at input intensities below  $2 \times 10^{17}\ \text{W cm}^{-2}$ . Such intensities are too low to trap and accelerate electrons. Here we report the first guiding of a relativistically intense laser ( $10^{19}\ \text{W cm}^{-2}$  input intensity) over a distance of  $10\ Z_R$ , and the resultant production of high-quality electron beams. Much as in a RF accelerator where cavities provide confinement and field shaping for the RF power, the plasma channel guides the laser beam and transversely shapes the plasma wakes.

The present experiments used the multi arm L'OASIS Ti:Sapphire laser<sup>22,23</sup>, operating at a wavelength of 810 nm with chirped pulse amplification<sup>24</sup>, to form a guiding channel<sup>18</sup> using a variation of the igniter-heater method<sup>19</sup> and to drive the plasma wake (Fig. 1). By adjusting the energy and the timing of the guide formation pulses, the channel profile was matched to guide the drive pulse without distortion over  $10\ Z_R$  at input powers up to 4 TW ( $7 \times 10^{18}\ \text{W cm}^{-2}$ ). Guiding efficiency at 4 TW was 35%, a reduction of 30% compared to the low-power case (0.5 TW), suggesting that a significant amount of laser energy was depleted by excitation of a plasma wave. No electrons were accelerated at 4 TW, offering the possibility of using laser injection<sup>16,17</sup> for the controlled trapping of electrons in this plasma wave without 'dark current'.

Electrons were trapped and accelerated using a 9 TW drive pulse, and optimal performance was found in channels detuned slightly from the low-power guiding condition, with 40% less rise in density over the spot diameter than a matched channel<sup>19</sup>. The contribution of relativistic self guiding present for the high-intensity pulse may be responsible for these changes. At 9 TW the mode image showed an intense output spot of  $24\ \mu\text{m}$  FWHM (Fig. 2b), slightly larger than the input spot but much smaller than the unguided pulse (Fig. 2d). Enlargement of the output spot compared to the input and leakage outside the guide appeared as the input intensity was increased well beyond the relativistic self focusing threshold, and are due to the inability of the channel to perfectly control the spot size in the presence of self guiding. Correlation of the mode imager and interferometer measurements showed that an intense guided mode was present only when the interferometer indicated that the laser was well confined to the channel (Fig. 2a). The axial plasma density was within 10% of  $1.9 \times 10^{19}\ \text{cm}^{-3}$  over the central 1.7 mm of the jet, and the drive laser pulse was thus a factor of two longer than the linear plasma period, that is, in the self-modulated regime<sup>6</sup>. This regime was chosen to allow comparison to unchannelled experiments, and also because the slower phase velocity of the wake at high plasma density allows trapping of background plasma electrons, yielding high-charge electron beams without a separate injector.

As shown in Fig. 3, the channel-guided accelerator produced

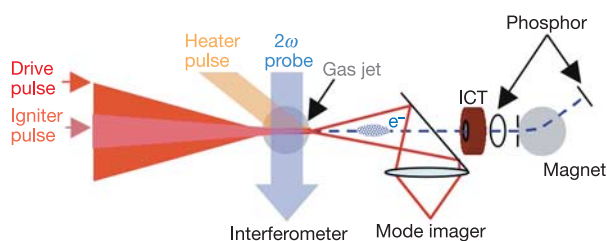


**Figure 1** In the channel-guided laser wakefield accelerator, the plasma channel was formed in a supersonic hydrogen gas jet by two pulses fired 500 ps before the drive pulse. The supersonic gas jet was 2.4 mm long at an atomic density of  $4.5 \times 10^{19}\ \text{cm}^{-3}$ . A cylindrical filament of plasma was ionized by an intense (60 fs, 15 mJ) igniter pulse, collinear with the pulse that drives the plasma wave and focused at  $1/5$  near the downstream edge of the gas jet. The plasma was subsequently heated to tens of eV by inverse bremsstrahlung, using a long (250 ps, 150 mJ) pulse incident from the side for efficient heating. The resulting hot plasma filament on axis expanded outward, driving a shock wave. This shock resulted in a density depletion on axis and a nearly parabolic transverse density profile which was tuned by adjusting the timing and energies of the beams. The plasma wave was driven by a 500 mJ pulse of 55 fs FWHM, focused at the upstream edge of the channel to an  $8.5\ \mu\text{m}$  FWHM spot by an  $f/4$  off axis parabola giving an intensity of  $1.1 \times 10^{19}\ \text{W cm}^{-2}$ . Propagation of the laser was monitored with a side interferometer (using a  $2\omega$  probe laser) and mode imager CCD. The electron beam accelerated by the plasma wave was analysed using an integrating current transformer (ICT), a phosphor screen, and a magnetic spectrometer ( $55^\circ$  bend angle used for high resolution at energy  $<92$  MeV,  $5^\circ$  for higher energies).

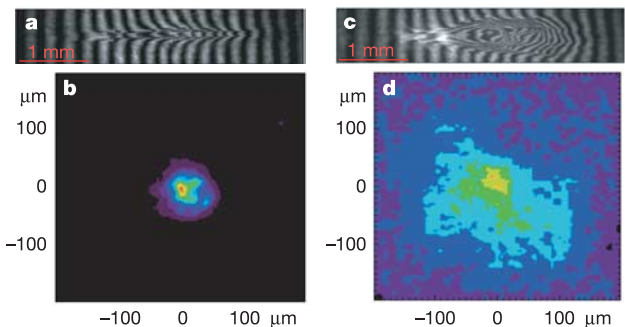


**Figure 2** Laser propagation with and without channel. The plasma size after the propagation of the drive pulse shows the radial extent of ionization, indicating the extent of diffraction of the laser as it propagates through the plasma. The profile of the laser spot at the exit of the plasma was viewed using a solid mirror inserted into the beamline and an  $f/10$  achromatic lens that imaged the laser spot directly onto a CCD (mode imager) camera providing  $10\ \mu\text{m}$  resolution. In the channel-guided accelerator, the plasma (a) was similar to the guiding channel indicating that the drive laser pulse was confined to the channel. The laser mode at the channel exit is a well defined spot of  $24\ \mu\text{m}$  FWHM containing 10% of the input energy (b). This indicates the effectiveness of the channel in maintaining the drive beam intensity and mode over many diffraction lengths. The spot is circular, confirming that the guiding channel is cylindrically symmetric. The reduction in energy from the input spot is due to a combination of leakage from the channel and depletion of the laser energy to excite the wake. When the channel was off, the interferometer showed blow out of the drive pulse after a few hundred micrometres (c), and the mode imager showed a diffuse transmitted spot (d).

high-charge electron beams with small energy spread at high energy, a unique feature that has not been observed in previous laser plasma acceleration experiments. To obtain the beam charge, the spectrometer phosphor screen has been calibrated against an integrating current transformer (ICT) and against radionuclide activation measurements<sup>9</sup>, both of which are consistent. For the data shown in Fig. 3, the  $\pm 2\%$  energy spread of the peak centred at 86 MeV is essentially limited by the spectrometer resolution, so that the beam may in fact have narrower energy spread. The divergence of the bunch at 86 MeV was half that of the integrated beam observed on the phosphor before the magnet, consistent with previous experiments that have shown that higher-energy electrons were more collimated<sup>2</sup>. The bunch shows a contrast ratio greater than 10:1 above a broad distribution of charge extending on either side. Space charge effects should be minimal for this relativistic beam, so assuming ballistic propagation from a source the size of the laser spot in the channel (8.5  $\mu\text{m}$  at entrance, 24  $\mu\text{m}$  at exit), an upper limit for the emittance can be obtained. Femtosecond bunches have hence been produced<sup>25</sup> containing  $2 \times 10^9$  electrons with geometric and normalized r.m.s. emittances  $\epsilon_x$  below 0.05–0.01  $\pi$  mm mrad and below 1–2  $\pi$  mm mrad r.m.s., respectively. The peak current is of the order of 10 kA with emittance comparable to the best state of the art RF facilities<sup>11</sup>. Bunches with energy up to 150 MeV have been observed on separate shots (see below).

Two-dimensional simulations using the particle in cell (PIC) code VORPAL<sup>26</sup> with parameters close to the experiment indicate that the high-quality electron bunches observed may be formed by a combination of pulse evolution, beam loading, and dephasing. As the drive laser pulse propagates through the plasma it self modulates, driving an intense plasma wake that traps electrons. The initial bunch of trapped electrons induces a secondary wake which interferes with the primary wake, reducing its amplitude<sup>27</sup>. If the drive laser pulse energy is just above the threshold for trapping, this beam loading effect suppresses further injection, creating an electron bunch isolated in phase space. The trapped electrons are then accelerated until they outrun (dephase from) the wake, at which point they are concentrated in phase and energy, forming a high-quality bunch with low energy spread (Fig. 4). Matching accelerator length and dephasing length to obtain high-quality bunches with the parameters (jet length and  $Z_R$ ) of this experiment required maintaining the intensity of the laser over many  $Z_R$  using a guiding

channel. This dephasing condition can alternatively be met by a short plasma at high density (see below) or by using a larger laser spot size to extend  $Z_R$ , but these alternatives are less efficient since high density lowers peak energy while large spot size requires many times greater laser power. Fluid<sup>28</sup> and other PIC<sup>29</sup> simulations have also observed that longer acceleration length results in narrow energy spread. Only one accelerating period of the plasma wave contributes to the high-energy beam due to beam loading in these simulations, so that the bunch length is less than a plasma period; for the experimental parameters the bunch length is near 10 fs FWHM.

The quality of optical guiding as well as the pointing, quality and charge of the electron beams at high energy fluctuated from shot to shot, probably caused by laser pointing jitter that changes the overlap between the wake drive pulse and the channel formation pulses (and hence guide quality and incoupling) as well as laser power fluctuations. Beams with  $3 \times 10^9$  electrons have been observed at similar energies ( $78 \pm 3$  MeV FWHM), and electrons were observed up to the limit of our 55° high-resolution spectrometer (92 MeV). Using a separate phosphor screen placed after the magnet at a 5° angle to the beam, we observed bunches at energies up to 150 MeV, but this diagnostic does not allow the fine resolution required to resolve energy spread. Structure in the energy spectrum has been seen for electrons with energy as low as 15 MeV. Below 15 MeV there is an essentially continuous distribution, and total beam charge was  $1.7 \times 10^{10}$  electrons as measured by the ICT, subtending  $f/8$ . Using a bend magnet, the low-energy contribution can be separated, leaving a high-energy, high-quality beam with a few times  $10^9$  electrons. Consistent control of guiding and electron injection<sup>16,17</sup> in order to stabilize these beams are among the next challenges for laser accelerators.

To provide a baseline for evaluating the effects of guiding, the accelerator was operated with the same gas jet and laser but without the guiding channel. As seen in Fig. 2c and d, the laser pulse diffracted strongly, limiting the acceleration length. The electron beam had a total charge of  $1.5 \times 10^{10}$  electrons, as measured by the ICT, with divergence near 50 mrad FWHM. The electron energy spectrum is described by a two-temperature Boltzmann distribution characterized by a 2.6 MeV temperature below 10 MeV and an 8 MeV temperature above 10 MeV. Structure in the energy spectrum did occur occasionally in the tail of the distribution above 15 MeV containing <2% of the charge, consistent with a beam accelerated over a short distance and with previous exper-

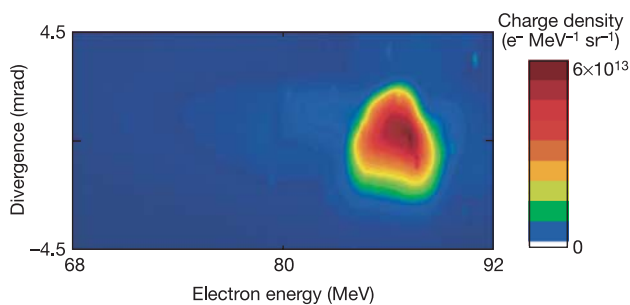


**Figure 3** Single-shot electron beam spectrum and divergence of the channel-guided accelerator, showing a bunch containing  $2 \times 10^9$  electrons in a narrow distribution at  $86 \pm 1.8$  MeV and 3 mrad divergence FWHM with contrast  $>10:1$  above background. This distribution is qualitatively different from the exponential distribution obtained in past (unchannelled) laser acceleration experiments. The magnetic spectrometer consists of a slit 82 cm from the gas jet, a bend of 55° in a dipole magnet to provide dispersion, and a phosphor screen (LANEX Fast backed by an aluminium foil to reject laser light) imaged by a CCD camera. Single-shot energy range is  $\pm 15\%$  about a central value selectable from 1 to 80 MeV, and resolution is  $dE/E = \pm 2\%$ . The vertical beam size is obtained in the undispersed direction, allowing the simultaneous determination of (vertical) divergence and energy. Since electron beams observed on the phosphor before the magnet were typically round in shape, this vertical divergence measurement is representative.

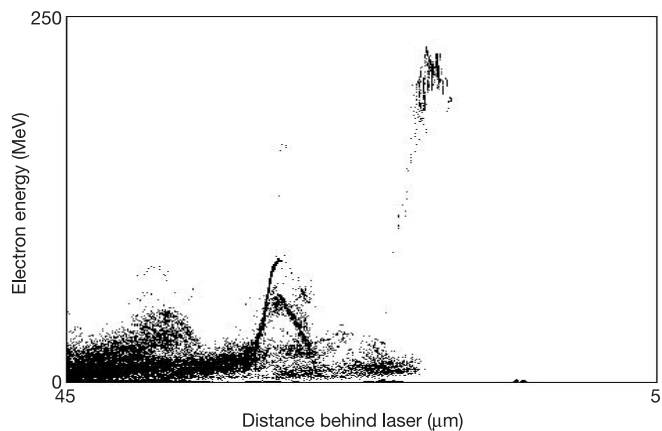


**Figure 4** Particle in cell simulations, here displaying the phase space of the electrons, show an energy distribution similar to that in the experiments. A high-quality electron bunch is formed when the acceleration length is matched to the dephasing length, and when the laser strength is such that beam loading is sufficiently strong to turn off injection after the initial bunch of electrons is loaded. The peak energy observed in the simulations is 200 MeV, close to the experimental result.

iments<sup>1,2,9</sup>. No electrons were observed above 40 MeV on the spectrometer phosphor screen (detection threshold  $10^7$  electrons). Plasma density was independently optimized for the unchannelled accelerator, and highest charge and electron energies were obtained at  $4 \times 10^{19} \text{ cm}^{-3}$ . The high density allowed acceleration before the laser diffracted since self modulation and dephasing both occur more quickly at high density, but this also reduced the peak energy compared to the channelled case. Operating the unchannelled accelerator at the density used for the channelled accelerator ( $2 \times 10^{19} \text{ cm}^{-3}$ ) produced low-charge low-energy beams, since the intensity of the drive beam was not maintained for sufficient distance to allow acceleration at this density without channelling. Using a 600- $\mu\text{m}$ -long plasma at  $4 \times 10^{19} \text{ cm}^{-3}$ , which is close to the dephasing length observed in PIC simulations at this density, the unchannelled accelerator produced the same peak energy as in the 2 mm plasma, but with more structure in the spectrum. These results confirm that matching accelerator length to dephasing length is critical for structuring the spectrum, and that extending the length (for instance, using a channel at lower density) results in higher energies.

To differentiate the effects of channelling from pre-ionization, the igniter pulse was fired 80 ps before the drive pulse. The plasma does not expand significantly over 80 ps, so there was no shock wave and the transverse density profile was flat and had no guiding properties. We observed no difference between the drive pulse only and pre-ionized cases, indicating that channelling and not pre-ionization was responsible for differences in the electron beams described above.

The beams from channel-guided accelerators such as those described here, with a few times  $10^9$  electrons in per cent level energy spread and mrad divergence, as well as intrinsic synchronization to the laser beam, open up a new class of experiments with laser accelerators. The channelling technology offers the ability to control the laser beam propagation much as a copper structure provides guiding and field shaping to RF accelerators. The investment of power in channel formation is less than 5% of the drive pulse power (20% of the energy), yet the spectral density of these beams near 80 MeV is at least a factor of 200 above previous unchannelled experiments using several times the laser power, and peak energy observed is comparable<sup>2</sup>. The narrow energy spread of the channel-produced beams is consistent with simulations, which also indicate that the bunch length is near 10 fs. The channel-guided laser accelerator technique will hence allow efficient generation of femtosecond X-rays<sup>10</sup>, coherent THz and infrared radiation<sup>13,30</sup>, and is an essential step towards the development of compact multistage electron accelerators with ultrafast bunches and with focusability and luminosity competitive with state of the art RF accelerators. □

Received 4 June; accepted 29 July 2004; doi:10.1038/nature02900.

1. Modena, A. *et al.* Electron acceleration from the breaking of relativistic plasma waves. *Nature* **377**, 606–608 (1995).
2. Malka, V. *et al.* Electron acceleration by a wake field forced by an intense ultrashort laser pulse. *Science* **298**, 1596–1600 (2002).
3. Leemans, W. P. *et al.* Electron-yield enhancement in a laser-wakefield accelerator driven by asymmetric laser pulses. *Phys. Rev. Lett.* **89**, 174802 (2002).
4. Tajima, T. & Dawson, J. M. Laser electron accelerator. *Phys. Rev. Lett.* **43**, 267–270 (1979).
5. Esarey, E., Sprangle, P., Krall, J. & Ting, A. Overview of plasma-based accelerator concepts. *IEEE Trans. Plasma Sci.* **24**, 252–288 (1996).
6. Esarey, E., Krall, J. & Sprangle, P. Envelope analysis of intense laser pulse self-modulation in plasmas. *Phys. Rev. Lett.* **72**, 2887–2890 (1994).
7. Esarey, E., Sprangle, P., Krall, J. & Ting, A. Self-focusing and guiding of short laser pulses in ionizing gases and plasmas. *IEEE J. Quant. Electron.* **33**, 1879–1914 (1997).
8. Najmudin, Z. *et al.* Self-modulated wakefield and forced laser wakefield acceleration of electrons. *Phys. Plasmas* **10**, 2071–2077 (2003).
9. Leemans, W. P. *et al.* Gamma-neutron activation experiments using laser wakefield accelerators. *Phys. Plasmas* **8**, 2510–2516 (2001).
10. Leemans, W. P. *et al.* Observation of terahertz emission from a laser-plasma accelerated electron bunch crossing a plasma-vacuum boundary. *Phys. Rev. Lett.* **91**, 074802 (2003).
11. Catravas, P., Esarey, E. & Leemans, W. P. Femtosecond x-rays from Thomson scattering using laser wakefield accelerators. *Meas. Sci. Technol.* **12**, 1828–1834 (2001).
12. Wang, X. J., Qiu, X. & Ben-Zvi, I. Experimental observation of high-brightness microbunching in a photocathode RF electron gun. *Phys. Rev. E* **54**, R3121–R3124 (1996).

13. Schoenlein, R. W. *et al.* Femtosecond X-ray pulses at 0.4 Å generated by 90° Thomson scattering — A tool for probing the structural dynamics of materials. *Science* **274**, 236–238 (1996).
14. Sprangle, P., Esarey, E., Krall, J. & Joyce, G. Propagation and guiding of intense laser pulses in plasmas. *Phys. Rev. Lett.* **69**, 2200–2203 (1992).
15. Leemans, W. P. *et al.* Plasma guiding and wakefield generation for second-generation experiments. *IEEE Trans. Plasma Sci.* **24**, 331–342 (1996).
16. Umstadter, D., Kim, J. K. & Dodd, E. Laser injection of ultrashort electron pulses into wakefield plasma waves. *Phys. Rev. Lett.* **76**, 2073–2076 (1996).
17. Esarey, E., Hubbard, R. F., Leemans, W. P., Ting, A. & Sprangle, P. Electron injection into plasma wake fields by colliding laser pulses. *Phys. Rev. Lett.* **79**, 2682–2685 (1997).
18. Durfee, C. G. & Milchberg, H. M. Light pipe for high intensity laser pulses. *Phys. Rev. Lett.* **71**, 2409–2412 (1993).
19. Volfbeyn, P., Esarey, E. & Leemans, W. P. Guiding of laser pulses in plasma channels created by the ignitor-heater technique. *Phys. Plasmas* **6**, 2269–2277 (1999).
20. Kim, K. Y., Alexeev, I., Fan, J., Parra, E. & Milchberg, H. M. Plasma waveguides: Addition of end funnels and generation in clustered gases. *AIP Conf. Proc.* **647**, 646–653 (2002).
21. Gaul, E. W. *et al.* Production and characterization of a fully ionized He plasma channel. *Appl. Phys. Lett.* **77**, 4112–4114 (2000).
22. Toth, C. *et al.* Powerful, pulsed, THz radiation from laser accelerated relativistic electron bunches. *Proc. SPIE* **5448**, 491–504 (2004).
23. Leemans, W. P. *et al.* Laser-driven plasma-based accelerators — Wakefield excitation, channel guiding, and laser triggered particle injection. *Phys. Plasmas* **5**, 1615–1623 (1998).
24. Strickland, D. & Mourou, G. Compression of amplified chirped optical pulses. *Opt. Commun.* **56**, 219–221 (1985).
25. Leemans, W. P. *et al.* Terahertz radiation from laser accelerated electron bunches. *Phys. Plasmas* **5**, 2899–2906 (2004).
26. Nieter, C. & Cary, J. R. VORPAL: A versatile plasma simulation code. *J. Comput. Phys.* **196**, 448–473 (2004).
27. Katsouleas, T., Wilks, S., Chen, S., Dawson, J. M. & Su, J. J. Beam loading in plasma accelerators. *Part. Accel.* **22**, 81–99 (1987).
28. Reitsma, A. J. W. *et al.* Simulation of electron postacceleration in a two-stage laser wakefield accelerator. *Phys. Rev. ST Accel. Beams* **5**, 051301 (2002).
29. Tsung, F. S. *et al.* Near GeV energy laser wakefield acceleration of self-injected electrons in a cm scale plasma channel. *Phys. Rev. Lett.* submitted.
30. Saes, M. *et al.* A setup for ultrafast time-resolved x-ray absorption spectroscopy. *Rev. Sci. Instrum.* **75**, 24–30 (2004).

**Acknowledgements** This work was supported by the US Department of Energy and the National Science Foundation and used resources of the National Energy Research Scientific Computing Center at LBNL; C.G. was also supported by the Hertz Foundation. C.G. acknowledges his faculty advisor J. Wurtele. We appreciate contributions from G. Dugan, J. Faure, G. Fubiani, B. Nagler, K. Nakamura, N. Saleh, B. Shadwick, L. Archambault, M. Dickinson, S. Dimaggio, D. Syversrud, J. Wallig and N. Ybarrolaza.

**Competing interests statement** The authors declare that they have no competing financial interests.

**Correspondence** and requests for materials should be addressed to W.P.L. (wplemans@lbl.gov).

## A laser-plasma accelerator producing monoenergetic electron beams

J. Faure<sup>1</sup>, Y. Glinec<sup>1</sup>, A. Pukhov<sup>2</sup>, S. Kiselev<sup>2</sup>, S. Gordienko<sup>2</sup>, E. Lefebvre<sup>3</sup>, J.-P. Rousseau<sup>1</sup>, F. Burgy<sup>1</sup> & V. Malka<sup>1</sup>

<sup>1</sup>Laboratoire d'Optique Appliquée, Ecole Polytechnique, ENSTA, CNRS, UMR 7639, 91761 Palaiseau, France

<sup>2</sup>Institut für Theoretische Physik, 1, Heinrich-Heine-Universität Duesseldorf, 40225 Duesseldorf, Germany

<sup>3</sup>Département de Physique Théorique et Appliquée, CEA/DAM Ile-de-France, 91680 Bruyères-le-Châtel, France

Particle accelerators are used in a wide variety of fields, ranging from medicine and biology to high-energy physics. The accelerating fields in conventional accelerators are limited to a few tens of MeV m<sup>-1</sup>, owing to material breakdown at the walls of the structure. Thus, the production of energetic particle beams currently requires large-scale accelerators and expensive infrastructures. Laser-plasma accelerators<sup>1</sup> have been proposed as a next generation of compact accelerators because of the huge